International Journal of Nanoelectronics and Materials
Volume 16 (Special Issue) December 2023 [73-86]

AuNPs/GO Coated U-Shape Polished SMF Based Localized SPR Sensor for Musta'mal Water Identification

Nur Zahirah Ahmad Khirri[1], Wan Maisarah Mukhtar[1,*], Razman Mohd Halim[2], Affa Rozana Abdul Rashid[1] and Nur Athirah Mohd Taib[1]

[1]Faculty of Science and Technology, Universiti Sains Islam Malaysia (USIM), 71800 Bandar Baru Nilai, Negeri Sembilan, Malaysia
[2]National Metrology Institute of Malaysia (NMIM), SIRIM Berhad, Bandar Baru Salak Tinggi, 43900 Sepang, Selangor, Malaysia

ABSTRACT

Potential of hybrid gold nanoparticles/graphene oxide (AuNPs/GO) coated single mode fiber (SMF) sensor by exploiting localized surface plasmon resonance (LSPR) effect for Musta'mal water identification was studied. Three structure shapes of fiber optics such as straight-shape, loop-shape and u-shape had been prepared. Three layers of AuNPs with 50 nm in diameter were drop-casted onto the partially unclad polished single mode fiber (SMF) to observe the maximum sensitivity of LSPR. To enhance the LSPR effect, one layer of GO was deposited on top of the AuNPs layer. Two optical light sources with least attenuation (1310 nm and 1550 nm) were employed to study the optical power output as the sensor immersed in different type of water samples. The u-shape SMF portrayed the maximum output power about 24.2 dBm at 1550 nm wavelength. According to the analysis, the deployment of 1550 nm laser wavelength resulted in better sensitivity with 23.2% improvement compared to 1310 nm wavelength. Apparently, the LSPR phenomenon created by AuNPs/GO able to enhance the plasmonic signal up to 51.9% than the uncoated SMF. The thinnest diameter of SMF's cladding, d=0.1195 mm with U-shape structure exhibited the highest power different of 1.10 dBm, in which suggested the best sensing performance. In conclusion, the optimization of AuNPs/GO u-shape polished SMF resulted in the maximum sensitivity with value of S=72.7 dBm/RIU for Musta'mal water identification.

Keywords: Gold nanoparticles (AuNPs), Graphene Oxide (GO), Localized Surface Plasmon Resonance (LSPR), polished SMF, Musta'mal, optical sensor

1. INTRODUCTION

Water is claimed as a fundamental resource to support humans and other creatures' survival. Unfortunately, water supplies around the world are expected to continue decline due to climate change. These limited water resources are increasingly threatened by the increment of population growth which is predicted to reach 8.9 billion by 2050. This will increase the water supply demand high quality for domestic purposes and economic activities in water-stressed countries. In Islamic perspective, water occupies pivotal role in performing worship [1]. An amount of water is used for ceremonial washes before Islamic prayer is known as Wudu' (ablution). In mosques, higher consumption of water is due to unhealthy behaviours of community that deliberately letting the water from the tap to flow for a long period and used large amount of water for purification. Apparently, this resulting in the increment of Musta'mal (used) water quantity in which leads to the increased of the usage of clean water for ablution. Then without being reused, the used water will flow back into natural environment. In mosques, higher consumption of water is due to unhealthy behaviours of community that deliberately letting the water from the tap to flow for a long period and used large amount of water for purification. The division types of water in Islamic view are only based on theoretical methods.

* Corresponding authors: wmaisarah@usim.edu.my

According to *Fiqh* perspective, a water taps less than two *qullahs* (not exceeding 270 litres) cannot be used for purification to perform worship [1]. The fact that water is essential element of the environmental sustainability and in humans' life, it is demanded to develop technologies that have high sensitivity of water quality identification.

Until today, most research works focused on the water quality in the environmental awareness aspects [2]. Enzyme sensors, electrochemical sensors, and piezoelectric sensors are among a few techniques that have been developed to identify the number of heavy metals, bacteria, and ions in wastewater [3-5]. These technologies do have some drawbacks, though, including their expensive price and complicated process. Optical sensors are one of the promising devices that offers outstanding features such as high sensitivity, excellent selectivity, straight-forwarded working principles and simple design [6,7]. Optical sensors can be divided into two categories which are fiber optics-based and free space optics-based [8,9]. Various types of fiber optics sensors have been developed such as by using common optical communication fiber optics including glass single mode fiber, plastic optical fiber, fiber Bragg grating and hybrid structure of fiber optics consists of combination of various types of fiber like single mode fiber-multimode fiber-single mode fiber (SMF-MMF-SMF) [10-14]. Apparently, each structure of fiber optics exhibited various sensitivity performance of the sensors.

Surface plasmon resonance is an optical phenomenon that occur as p-polarized light interacts with noble metal such as gold and silver. The output of this phenomenon results excitation of surface plasmon polaritons (SPP) that will enhance the strength of evanescence field [15]. SPR phenomenon has been widely used in sensing and optoelectronics applications [16, 17]. The introduction of additional materials such as graphene oxide exhibits an outstanding performance in which strong SPR signal is successfully generated [18, 19]. Other than that, by manipulating the physical structure of the metal coated fiber itself, the sensitivity of SPR-based fiber optics sensors has shown significant enhancement on their sensing characteristics [2, 20-22].

Based on the previous works by other researchers, it can be concluded that localized SPR is a popular sensor for water quality identification due to its high sensitivity, simple structure and portable. In term of sensing application for the ablution purpose, it is found that previous studies focused on the development of recycling device for reusing ablution water which involve few sensors such as ultrasonic sensors and other indicator sensors. Lack of studies for the sensor's development to identify the quality of water for ablution motivate the author to propose this work. Therefore, this study proposed the development of simple and high responsivity optical sensor utilizing gold nanoparticles and graphene oxide (Au/GO) coated on u-shape single mode fiber (SMF) in generating strong localized surface plasmon resonance (LSPR) for Musta'mal water identification. We believe the output of this study will contribute to the technology development for the benefits of Muslim community.

2. MATERIAL AND METHODS

2.1 Fabrication of Partially Unclad Fiber via Mechanical Polishing Approach

The experiment used a single mode optical fiber (SMF) with diameters of core and cladding were 9 μm and 125 μm respectively. About 1 meter long of SMF was used to prepare five samples of the polished fiber. Approximately ~ 4 cm length of SMF was unjacketed by using fiber stripper to remove the polymer buffer coating and to expose the bare region. The bare area of the five fiber samples were cleaned with ethyl alcohol before the mechanical polishing process. A P2000 grit sandpaper (Brand: Neitz) with the smallest and the finest abrasive particles was used for fiber polishing since it was intended for surface smoothing.

The polishing technique was implemented by using the sandpaper to reduce the SMF cladding diameter of the bare area. Note that this technique was performed manually by repeating five times for each number of polishing. The first sample was maintained the original size of cladding without getting any polished (n = 0). The second sample of fiber was polished once (n = 1), the third sample was polished two times (n = 2), three polishes were made with the fourth fibre sample (n = 3), and the last fiber sample was polished four times ((n = 4). A careful handling was required when the number of swipes increased. The physical structures of these samples were characterized using optical microscope (Brand: Mitutoyo) and optical profilometer (Brand: Bruker – ContourGT).

Next, the effect of fiber's shapes such as straight-shape, loop-shape and u-shape on the optical output power was investigated by manually bending the fibers. Figure 1 depicts three different shapes designed on SMF namely (a) straight-shape, (b) loop-shape and (c) u-shape. Note that the diameter of both loop-shape and u-shape were maintained at d = 8 cm considering this is the critical minimum macrobending diameter before the fiber started to fracture. The formation of macrobend structure will excite the evanescent waves that consequently become one of the main factors to develop the sensing properties of the proposed sensor [22, 23]. The optical output power for each type of SMF shape was investigated to determine the optimum shape of the fiber with low optical losses. The percentage difference of diameter reduction for tapered fibers were measured using Equation (1) as follow:

$$Percentage\ difference\ (\%) = \left|\frac{d_f - d_i}{d_i}\right| \times 100 \quad (1)$$

where d_i is the initial diameter of unpolished cladding, while d_f is the final diameter of the polished fiber with frequency of polishing from one to four times.

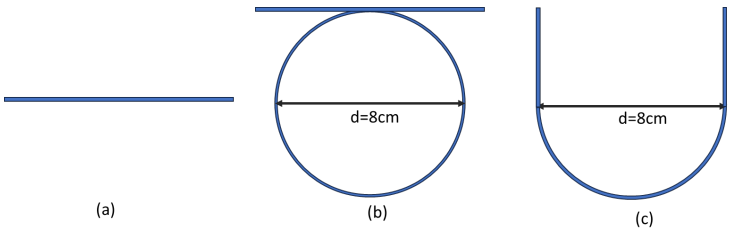

Figure 1. Three different shapes of SMF (a) straight-shape, (b) loop-shape and (c) u-shape.

2.2 Deposition of AuNPs/GO on the Substrate by using Drop-Casting Technique

Before performing deposition procedure, the AuNPs with average diameter size of 50 nm (commercially available) and graphene oxide (commercially available) were characterized using UV-Vis and FESEM analyzers to determine their morphological and optical characteristics. The experiment was continued by depositing gold nanoparticles/graphene oxide (AuNPs/GO) onto the optimized shape of SMF using drop-casting technique (Figure 2). The technique was performed on the 2 cm of the unjacketed polished region SMF (Fig. 2(a)). First, a droplet of 20µL AuNPs in the form of aqueous solution has been deposited onto the bare region. To ensure it was perfectly dried and attached on the SMF, it was left for an hour at room temperature for evaporation process. This procedure resulted in the formation of one layer of AuNPs on the SMF (Fig. 2(b)). This step was subsequently repeated by increasing the number of layers of AuNPs to two and three layers. Next, 20 µL of GO with concentration of 0.4% (Brand: Graphenea) was coated onto the AuNPs layers. The sample was then left for two hours at room temperature to establish the attachment of GO on the AuNPs coated SMF (Fig. 2(c)). It is noteworthy to highlight that the purposes of depositing AuNPs onto the substrate were to stimulate the LSPR and to

improve the sensing capabilities of the SMF sensor. Fig. 2(d) illustrates the AuNPs and GO layers that were successfully coated on the SMF by using drop-casting technique.

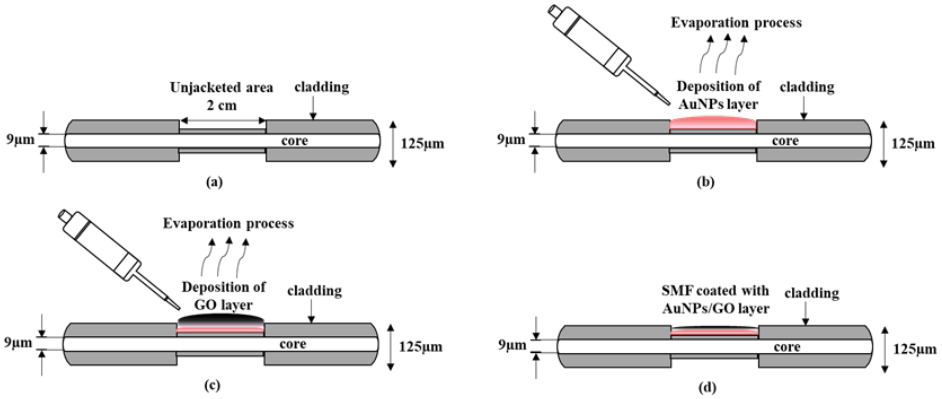

Figure 2. Overall process of drop-casting for AuNPs/GO deposition (a) Polished part of SMF, (b) Deposition of AuNPs on the polished SMF, (c) Deposition of GO on the polished AuNPs coated SMF, (d) AuNPs/GO were coated on the polished SMF.

2.3 Experimental Setup of the AuNPs/GO Fiber Optic LSPR Sensor for Musta'mal Water Identification

Three types of water sample were used in this work such as tap water, ablution tank's water and Musta'mal water of prayers. Distilled water was used as a reference reading. The experimental setup of the AuNPs/GO fiber optic LSPR sensor for Musta'mal water identification was developed by connecting both fiber ends to the infrared (IR) laser source (Brand: Noyes AFL with wavelength selection of λ_1=1310nm and λ_2=1550nm) and optical power meter (OPM) (Brand: Noyes AFL) respectively. Then, the coated AuNPs/GO sensing region with n=0 was immersed into different water samples that were stored in beakers. The same procedures were repeated for different cladding of tapered region of SMF ranging from n=1 to n=4. Next, the ideal design of the proposed sensor was evaluated throughout the research based on the observation of optical output power as the diameter of the fiber were modified. Lastly, the optical performance of each shape was measured by using Equation (2) to determine their sensitivity:

$$Sensitivity, S\ (dBm/RIU) = \frac{P_d - P_a}{|RI\ in\ distilled\ water - RI\ in\ air|} \times 100 \quad (2)$$

where, P_d is the optical power output of the shaped fiber as immersed into the distilled water while P_a is the optical power output of the fiber in air.

3. RESULTS AND DISCUSSION

3.1 Effect of Polishing Frequency to the Diameter of SMF

Figure 3 displays the image of the original size of the SMF's unpolished part (n=0). By using optical profilometer, the step height of unpolished bare area and its surface roughness at 0.125 mm was successfully observed indicating a good agreement with the manufacturer's measurement. Figure 4 depicts the images of different diameters of SMF under optical microscope where, (a) d=0.1250 mm for n=0, (b) d=0.1215 mm for n=1, (c) d=0.1210 mm for n=2, (d) d=0.1200 mm for n=3 and (e) d = 0.1195 mm for n=4. This research emphasized the employment of the finest abrasive sandpaper to reduce cladding thickness diameter as well as to create a coarser surface for adhesion of AuNPs and GO on the substrate. Figure 5 illustrates the linear correlation between fiber cladding's diameters and their frequency of polishing. The cladding diameter was effectively

decreased as higher frequency of polishing applied on the SMF with standard deviation for five trials per sample of the measurement up to $1x10^{-4}$ mm as displays in Fig.5(a) while the percentage difference of diameter's reduction between them shows an upward trend (Fig.5(b)). At n=1, 2.8% of the cladding region was satisfactorily polished from 0.1250 mm to 0.1215 mm. The cladding diameter was effectively decreased to 0.1210 mm which is 3.2% reduction from its original size at n=2. The reduction of cladding diameter by roughly 4.0% due to the increment in polishing number, n=3 resulted in d=0.1200 mm. When the polishing frequency reached n=4, the cladding's diameter decreased about 4.4%, producing in d= 0.1195 mm. From n=0 to n=1, a very significant decrease was obtained with difference of 0.0035 mm, while with every polish increment from n=1 to n=4, it shows consistent reduction of about 0.0005 mm. Considering the difficulty in controlling an unreliability factor of consistent stress on fiber, the frequency limit of swipes was limited to four times only. It was impracticable to polish the cladding fiber as n>4 through the mechanical polishing technique due to the fragility of the fiber that has a high tendency to rupture. There is a limitation in this approach, where the user could be overly cautious and unable to apply enough pressure while polishing that consequently will restrict the fabrication of fully unclad SMF. However, this approach has the advantage of being rather simple and cheap in comparison to other alternative tapering processes [6, 23].

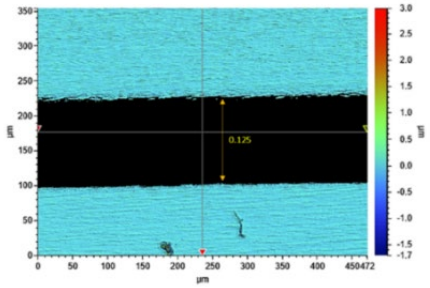

Figure 3. Step height analysis of fiber sample with no swiping (n=0) using profilometer.

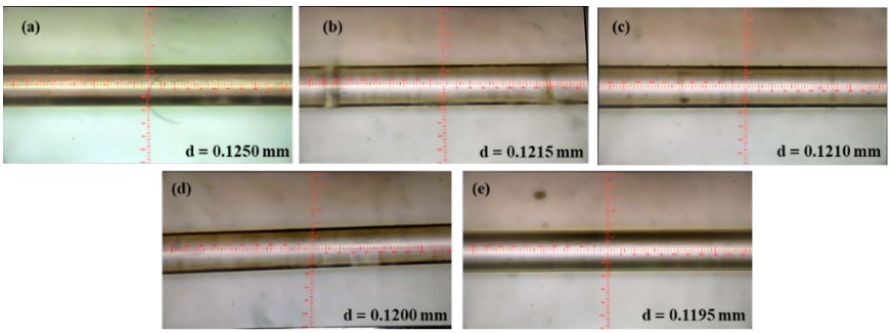

Figure 4. Macroscopic images of different diameter of the cladding; (a) d=0.1250 for n=0, (b) d= 0.1215 mm for n=1, (c) d=0.1210 mm for n=2, (d) d=0.1200 mm for n=3, (e) d = 0.1195 mm for n=4; using optical microscope.

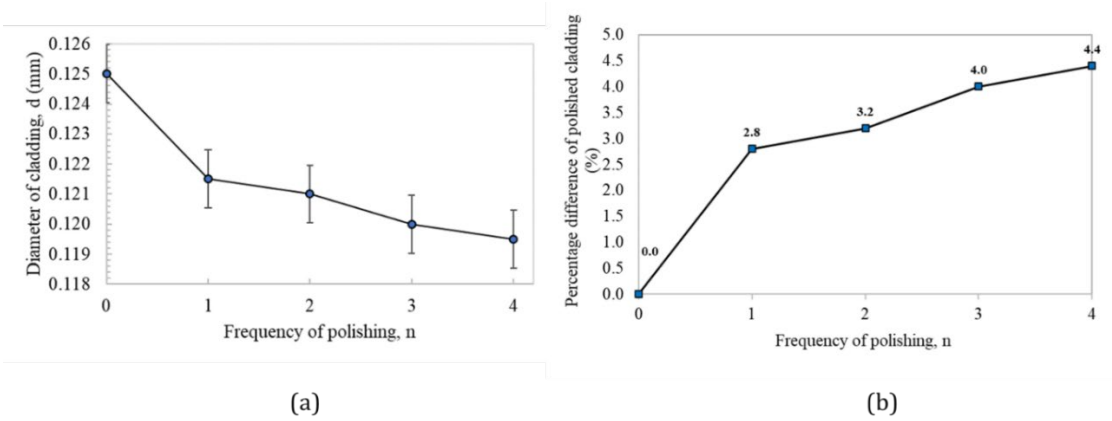

Figure 5. (a) Cladding's diameter decreased linearly as higher frequency of polishing were applied, n (b) Percentage difference of cladding's diameter reduction based on polishing frequency, n.

3.2 Characterization of AuNPs and GO: Morphology and Optical Characteristics

Figure 6 illustrates the UV-Vis spectroscopy characterization for different layers of 50 nm diameter size of gold nanoparticles colloidal that were drop-casted on the glass substrates, ranging from single drop to three drops. The maximum absorbance peaks of those samples were observed to appear at the wavelengths around 520 nm until 590 nm with the highest value located at 555 nm. This analysis led to the discovery that three droplets of colloidal gold can efficiently generate the strongest LSPR with 0.067 a.u. The absorption value were declined about 16.4% and 44.8% as light radiated on both two layers (0.056 a.u) and one layer (0.037 a.u) of AuNPs samples respectively. Based on the drop casting technique used, it was found that an additional layer of AuNPs can enhance the plasmonic effect. In this research, three layers of AuNPs were observed as the most optimal layer that can stimulate the LSPR phenomenon. Taking this into account, the possibility of AuNPs/GO partial unclad SMF as a sensing device was studied further by retaining three layers of AuNPs and modifying the diameter of fiber's cladding from n=0 to n=4.

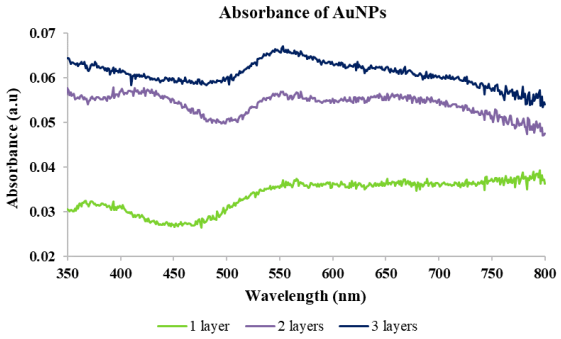

Figure 6. UV-Vis spectroscopy characterization for various layers of AuNPs drop-casted on glass substrates.

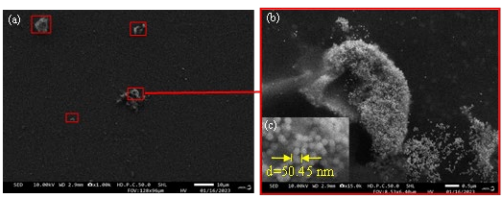

Figure 7. One drop of AuNPs under FESEM at different magnifications where, (a) at x1.0k, (b) at 15.0k and (c) at x200k.

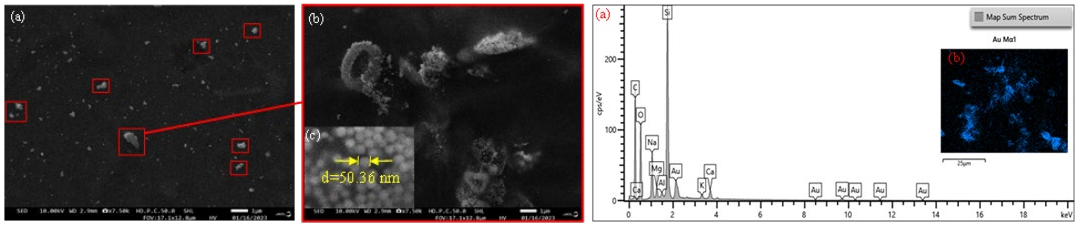

Figure 8. Three drops of AuNPs under FESEM at different magnifications where, (a) (i) at x1.0k, (ii) at 15.0k and (iii) at x200k (b) EDX analysis of three layers of AuNPs.

Figure 7 depicts the FESEM image of one drop of AuNPs deposited on the substrate using drop casting technique at different magnifications of (a) x1.0k, (b) 15.0k and (c) x200k. For one droplet of AuNPs, the nanoparticles were detected only clustered in few spots. 11 diameter readings of different nanoparticles were measured with the mean average of their size is about d= 50.45 nm. The smallest and largest size recorded are 49.22 nm and 52.20 nm. The range distance between them was roughly about L=8.92 nm with the shortest and longest length are L=5.00 nm and L=13.53 nm. Additionally, the images of three droplets of AuNPs at (a)(i) x1.0k, (ii) 15.0k and (iii) x200k magnifications are shown in Figure 8. For three droplets of AuNPs colloidal, a mean average of the diameter for 11 distinct nanoparticles was observed to be at d= 50.36 nm with minimum and maximum size are 49.01 nm and 51.12 nm. They were separated by approximately L=11.48 nm with the smallest and greatest lengths in their range were L=8.24 nm and L=15.19 nm, respectively. Observation of the AuNPs diameter range between one drop to three drops were comparable in which both were within 50 nm in diameter. This finding is aligned with the commercially available gold nanoparticles' diameter manufactured by Sigma-Aldrich. As the gold layer increased to three layers, it was found that the nanoparticles were clustered in more than six spots. It is noteworthy to highlight that the 50 nm diameter of AuNPs have been proved able to excite the strongest localized SPR among other sizes (10 nm – 100 nm) due to oscillations of electron cloud on the particle surface and the absorption of electromagnetic radiation at a particular energy [22]. Figure 8(b) illustrates the EDX analysis of three layers of AuNPs deposited on the substrate. Other elements (Si, In, Sn, Na, Mg, and Ca) were the components of silica glass substrate [23]. This output shows a good agreement with the UV-Vis spectroscopy results and strengthens the hypothesis that the additional layers of AuNPs have greater number of nanoparticles and possess higher absorbance. The topographical of GO under FESEM at magnification of x15.0k is shown in Figure 9. Although the drop-casting offers simple and less cost technique, one of its drawbacks is the formation of non-uniform film. As GO has been demonstrated to be capable of increasing the sensitivity of LSPR optical sensor, its thickness' uniformity significantly affected the sensing characteristics due the absorption of plasmons by the GO itself. Apparently, the presence of GO thin film influenced the change of power loss in which validated its significance in maximizing the optical performance of the polished SMF.

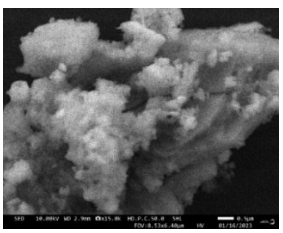

Figure 9. Topographical of GO under FESEM at magnification of x15.0k.

3.3 Analysis of Various Types of Water Samples

Table 1 describes the visual characteristics of four different water samples (distilled water, tap water, tap water and musta'mal water) that had been collected in this study. It should be noted that the distilled water served as a reference sample in this observation, while the rest of another sample was used as a manipulated variable. The findings found that musta'mal water had modifications in colour, odour and sediment compared to the other three water samples. Based on the observation of the natural senses of a human being, distilled water, tap water and tank water showed the same characteristics as each other which were clear in colour, odorless and no sediments produced. Meanwhile, the musta'mal water showed a contradictory characteristic in which its colour looked more murky or cloudy. This water also had a musty smell and sediment in it. The resulting sediment, water discoloration and unpleasant odour were expected due to the presence of saliva and plaque from the mouth when gargling, sweat and dirt on the skin as well as mucous when cleaning the nose. This output was in line with the point of view of sharia and Islamic perspective, where the ruling of musta'mal water is sacred but can no longer purify due to the change in the nature of the water, which are the color, smell and taste [1].

Table 1 Characteristics of different water samples

Description	**Water Samples**			
	Distilled Water	**Tap Water**	**Tank Water**	***Musta'mal* Water**
Colour	Clear	Clear	Clear	Cloudy
Odour	Odourless	Odourless	Odourless	Musty
Sediment	No	No	No	Yes

3.4 Sensitivity Analysis of Various Shapes of SMF Based on Macro Bending Effect

Table 2 indicates the optical power output (dBm) readings of various shapes of fibers in air and distilled water with two different laser excitation wavelengths, which were 1310 nm and 1550 nm. Figure 10 shows the overall sensitivity of different fiber's shape as light transmitted in air with RI=1.00 at different wavelengths of 1310 nm and 1550 nm, analyzing from the data obtained in Table 2. The loop-shape appeared to have the lowest sensitivity which are 9.1 dBm/RIU at 1310 nm and 12.1 dBm/RIU when projected with 1550 nm laser source. As the fiber was structured into straight shape, the fiber's sensitivity seems to be maintained at 12.1 dBm/RIU for 1550 nm whereas it showed an increment of 18.2 dBm/RIU when 1310 nm was utilized. The sensitivity rises in both lasers' excitation with 21.2 dBm/RIU and 24.2 dBm/RIU when the polished region was designed into u-shape. The entire data shows that at the wavelength of 1310 nm, the output power readings appeared to be higher than 1550 nm. This condition indicated that the deployment of 1550 nm as light source resulted in more sensitive and better efficiency in light transmission due to the lower power attenuation [24]. Overall, these findings indicated that the u-shape SMF was the most stable and possessed greater sensitivity compared to other shapes. This outcome is comparable to the result from Xie et al. (2020) concluded that the sensitivity of the sensor was significantly enhanced as the straight fiber was bent into a u-shape. Throughout this research, the design of the sensing region was retained in the form of u-shape and further observations were performed by considering the changing factors of the coating materials and the diameter of fiber's cladding.

Table 2 Power output (dBm) of various shape of fibers without getting any swipe (n=0) and without material's coating at 1310 nm and 1550 nm in air and distilled water

Fiber's Shape	ʎ = 1310 nm		ʎ =1550 nm	
	Power in Air, P_r (dBm)	Power in distilled water, P (dBm)	Power in Air, P_r (dBm)	Power, in distilled water P (dBm)
Loop-shape	2.9	2.93	1.82	1.86
Straight-shape	2.4	2.46	1.5	1.54
U-shape	2.86	2.93	1.82	1.9

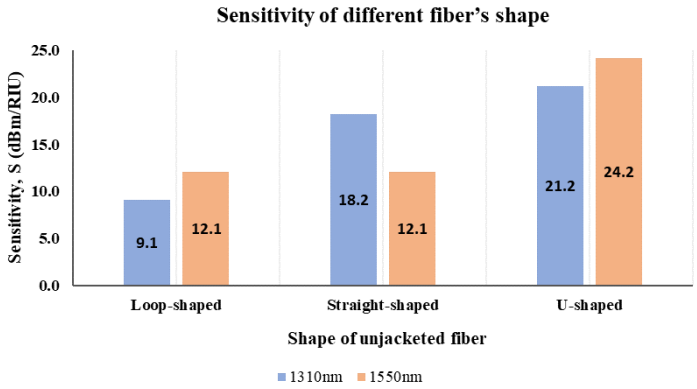

Figure 10. Sensitivity analysis of different fiber's shape using light operation wavelength of 1310 nm and 1550 nm as exposed in air.

3.5 Sensing Characterization of AuNPs/GO Coated on U-Bent Polished SMF in Identifying Musta'mal Water

Figure 11 indicates the value of optical output power when laser source with λ=1310nm was transmitted through the u-shaped SMF sensor. Fig. 11(a) and (b) shows the relationship between optical power output of 1310 nm against the cladding diameter as the uncoated and AuNPs coated SMF sensors were immersed into the three different types of water samples i.e. tap water, tank water and musta'mal water. The optical power output of all water samples in uncoated and AuNPs/GO coated SMF at λ=1310nm were observed to be dropped significantly from d=0.1250 mm to d=0.1210 mm and gradually rise back until d=0.1195 mm. This power drop condition occurred due to the light leakages as part of the transmitted light was radiated away from the partially unclad polished fiber in a form of evanescent waves. A fluctuation reading was obtained in both uncoated and coated SMF using the original size of the fiber with operating wavelength of λ=1310nm. In Fig. 11(a), the maximum output powers were obtained as the thinnest diameter of cladding, d=0.1195 mm was immersed into the three water samples. As for the tap water, it had a maximum optical power output P_t=3.05 dBm, while tank water and musta'mal water showed maximum output power of P_k=3.07 dBm and P_m=3.14 dBm respectively. Similar trend was obtained from the observation of AuNPs/GO coated fiber optic sensor as it was immersed into various water samples (Fig. 11(b)), where the maximum readings were found at d=0.1195mm with P_t=4.07 dBm, P_k=4.10 dBm and P_m=4.19 dBm respectively. Note that its selectivity capability in distinguishing different types of water became more significant with the addition of AuNPs and GO layers where the difference in output power between the three samples increasingly noticeable compared to the uncoated SMF.

Figure 12 illustrates the optical signal output of u-shaped SMF sensor as using laser excitation with λ=1550nm. Significant changes can be observed as the fiber coated AuNPs/GO (Fig. 12(b)) resulted greater output power compared to the uncoated fiber (Fig. 2(a)). This condition indicated the localized surface plasmon resonance excitation resulted in better sensitivity in detecting the presence of dust and particles in the water samples. It is noteworthy to mention that the main principle of optical sensor is based on the detection refractive index of the surrounding medium. The presence of large amount of dust, particles and contaminants in musta'mal water compared with others will cause only small portion of light to be radiated away from the fiber in which produced greatest output power among the others [22]. Note that the same pattern also can be seen as λ=1310 nm was operated (Figure 11). The efficiency of the sensor was examined based on a significant different value of the output power reading as it was immersed into the water samples and the variation of cladding diameter with deposition of additional materials. The correlation between the optical power output and the thicknesses of tapered sensing region is shown in Fig. 8(a) for uncoated SMF and Fig. 8(b) for AuNPs/GO coated SMF sensor. It was recorded that in both coated and uncoated AuNPs/GO SMF, optical power output of all water samples at 1550 nm dramatically decreased between d=0.125 mm and d=0.1215 mm before progressively increasing again until d=0.1195 mm. The trend of this non-linear data was comparable to the results at 1310 nm for both states of the constructed device. However, there were disproportionate fluctuations in unpolished fiber when the 1310 nm laser was deployed as shown in Fig. 11(a) and (b). It was found that the readings of the sensor with d=0.125 mm before and after being coated are unstable at 1310nm for all water samples. At 1550 nm, the maximum output powers of uncoated and AuNPs/GO coated fiber in the three water samples, was observed as the thinnest diameter of cladding, d=0.1195 mm was used. As the uncoated SMF with highest frequency of swiping was immersed in the samples, the maximum optical power output of tap water is P_t= 1.91 dBm, while those tank water and musta'mal water was observed to obtain P_k=2.03 dBm and P_m=2.12 dBm respectively. This upward trend recurred when the reading was taken by using AuNPs/GO coated fiber sensor, where the maximum value of optical power output for tap, tank and musta'mal water were P_t= 2.94 dBm, P_k=3.10 dBm and P_m=3.22 dBm correspondingly. Other sizes of fiber cladding did not show any significant changes in optical reading for the three water samples. In sum, in characterizing the musta'mal water, the AuNPs/GO coated SMF exhibited the maximum output power using the light operation wavelength of 1550 nm with 23.2% improvement compared to 1310 nm of wavelength.

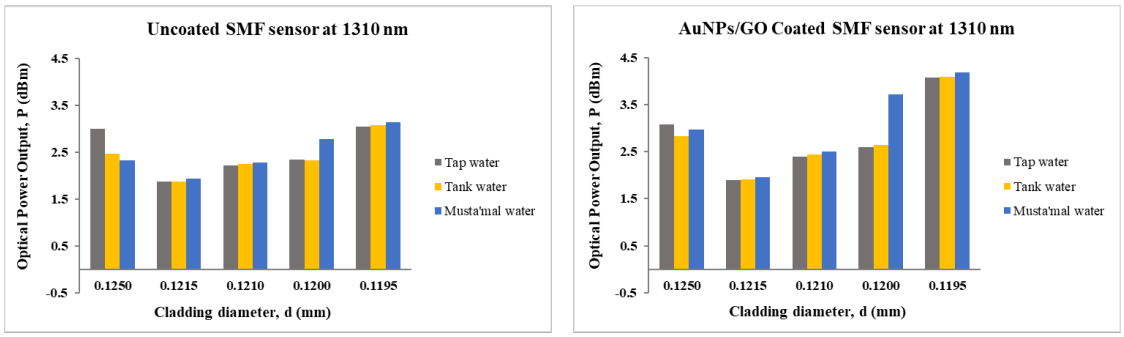

(a) (b)

Figure 11. (a) Optical output power of Uncoated SMF sensor at 1310 nm and (b) optical power output of AuNPs/GO Coated SMF sensor at 1310 nm.

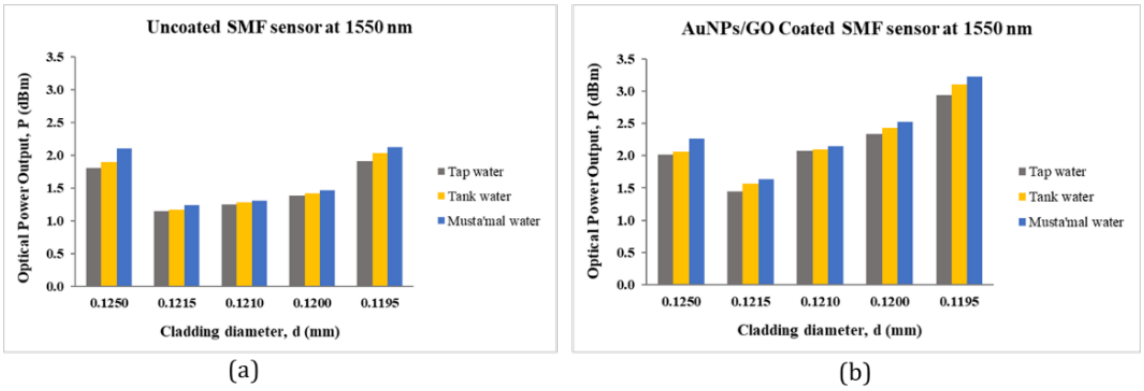

Figure 12. (a) Optical output power of Uncoated SMF sensor at 1550 nm and (b) optical power output of AuNPs/GO Coated SMF sensor at 1550 nm.

Figure 13 illustrates the power differences between uncoated and AuNPs/GO coated u-shape SMF in detecting three water samples. The sensitivity of the fabricated sensor was observed based on the changes amount of optical output power as different types of water were used. As 1310 nm light was transmitted, the maximum power difference, ΔP of tap water (ΔP_t), tank water (ΔP_k) and musta'mal water (ΔP_m) were observed with the fiber's diameter was set at d=0.1195 mm. Note that this diameter corresponded to the size of the SMF sensor that experienced the frequency of polishing process of n=4. The maximum power difference of each sample was obtained as ΔP_t=1.02 dBm, ΔP_k=1.03 dBm and ΔP_m=1.05 dBm respectively. At 1310 nm, the fiber sensor with the thinnest diameter portrayed excellence performance in detecting musta'mal water with regards to the highest ΔP with the increment of sensitivity about 8.25 % from the reference reading (DI water). As the wavelength increased to 1550 nm, the thinnest diameter exhibited the highest power difference in all water samples with ΔP_t=1.03 dBm, ΔP_k=1.07 dBm and ΔP_m=1.10 dBm. This situation shows greater improvement of sensitivity about 64.55 % compared to the distilled water. Obviously, the utilization of 1550 nm wavelength resulted in the sensitivity enhancement about 87.22 % compared to 1330 nm. This situation can be explained due to the large attenuation contributed by 1330 nm wavelength as its propagated inside the glass SMF, in which caused by the interaction between light and water molecule inside the fiber itself [24]. Note that the readings for tap and tank water did not show significant trend to each other compared to musta'mal water. It can be concluded that as the ablution water tank exceed 2 *qullah* which is more than 270 litres, the characteristic between them became comparable. At this point, tank water can be considered as mutlak water. Hence, it can be used for the purification purpose. Meanwhile, musta'mal water had portrayed the highest power changes due to its significant in power differences compared to other water samples. This may be due to the presence of greater number of pollutants or dusts in it which decreased the strength of evanescent field around the sensing region of the AuNPs/GO SMF that consequently led to the higher output power.

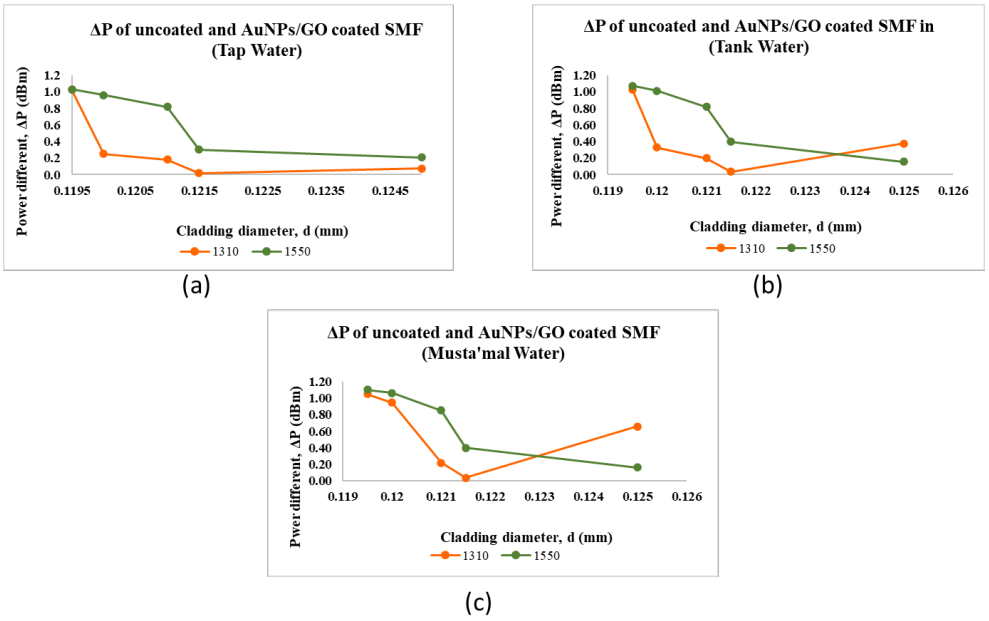

Figure 13. Power different, ΔP between uncoated and AuNPs/GO coated u-shape SMF in three water samples where (a) tap water (ΔP_t), (b) tank water (ΔP_k) and (c) musta'mal water (ΔP_m).

Table 3 lists the sensitivity values of the polished fiber with 0.1195 mm of cladding diameter in comparison between uncoated SMF and AuNPs/GO coated u-shape SMF at λ=1310nm and λ=1550nm for musta'mal water identification. The sensitivity of the SMF sensor in both conditions was calculated by using the Equation (2). In general, the sensing ability of the proposed optical system was enhanced with the introduction of additional materials. At 1310 nm, the sensitivity of uncoated SMF exhibited the lowest value with S = 24.24 dBm/RIU. As the fiber was replaced with AuNPs/GO coated SMF, the value of sensitivity increased by 75% with S = 42.42 dBm/RIU. The deployment of light with operation wavelength of 1550 nm laser witnessed the enhancement of laser's sensitivities. For the uncoated SMF, the sensitivity increased up to 12.5 % resulted the value of sensitivity as S=27.27 dBm/RIU compared to 1310 nm. The introduction of localized SPR using AuNPs/GO coated u-shape SMF significantly enhanced the sensitivity of the proposed sensor to S=72.73 dBm/RIU with 71.50 % of improvement for the musta'mal water identification. It is noteworthy to mention that the sensitivity of this sensor was also affected by the proper alignment between the incident light and SMF, which also helped to minimize the light attenuation issue.

Table 3 Sensitivity of tapered fiber with d=0.1195 mm in comparison between uncoated u-shape SMF and AuNPs/GO coated u-shape SMF at λ=1310nm and λ=1550nm

Wavelength	1310 nm		1550 nm	
	Uncoated SMF	AuNPs/GO coated SMF	Uncoated SMF	AuNPs/GO coated SMF
Power in Air, P_a (dBm)	3.06	4.05	2.03	2.98
Power in Musta'mal water, P_m (dBm)	3.14	4.19	2.12	3.22
Sensitivity, S (dBm/RIU)	24.24	42.42	27.27	72.73

4. CONCLUSION

In conclusion, there are many factors that need to be taken into consideration to develop highly sensitive optical fiber sensors including fiber's shape, fiber's structure such as diameter of cladding, light operation wavelength and coating materials. The output of this study shows that the usage of u-shape SMF with the diameter of polished cladding, d=0.1195 mm and operating wavelength of 1550 nm resulted in better sensitivity with 14.16 % of improvement, where the value was obtained as S = 21.20 dBm/RIU compared to the 1330 nm sensing system. Clearly, combination of localized plasmonic generated by AuNPs/GO and strong evanescence field produced by the macrobend partially unclad polished fiber was successfully enhanced the sensor's sensitivity up to 71.50 % in identifying musta'mal water. We believe the output of this study will contribute to the technology development for the benefits of Muslim community.

ACKNOWLEDGEMENTS

The authors would like to acknowledge the Faculty of Science and Technology, Universiti Sains Islam Malaysia (USIM) and National Metrology Institute of Malaysia (NMIM) for the research facilities.

REFERENCES

[1] Wan Zahari, W. A. M. (2021). Turkish Journal of Computer and Mathematics Education (TURCOMAT), vol **12**, issue 2 (2021) pp. 594–603.
[2] Mukhtar, W. M., Latib, S. N., Halim, R. M., & Rashid, A. R. A. Solid State Phenomena, vol **307** (2020) pp. 78–83.
[3] Alvarado-Ramírez, L., Rostro-Alanis, M., Rodríguez-Rodríguez, J., Sosa-Hernández, J. E., Melchor-Martínez, E. M., Iqbal, H. M., & Parra-Saldívar, R. Biosensors, vol **11**, issue 11(2021) pp. 410.
[4] Liu, Y., Xue, Q., Chang, C., Wang, R., Liu, Z., & He, L. Analytical Sciences, vol **38**, issue 1(2022) pp. 55-70.
[5] Insabella, R. M., González, M. G., Acosta, E. O., & Santiago, G. D. Measurement Science and Technology, vol **31**, issue 12 (2020) pp. 125103.
[6] Rashid, A. R. A., Nasution, A. A., Suranin, A. H., Taib, N. A., Mukhtar, W. M., Dasuki, K. A., & Ehsan, A. A, "Chemical tapering of polymer optical fiber", in International Conference on Applied Photonics and Electronics 2017 (InCAPE2017), Malaysia, (2017) pp. 01015.
[7] Menon, P. S., Gan, S. M., Mohamad, N. R., Jamil, N. A., Tarumaraja, K. A., Razak, N. R., Mukhtar, W.M., Murat, N.F., Mohamed, R., Khairulazdan, & Said, F. A., "Kretschmann based surface plasmon resonance for sensing in visible region", in *2019 IEEE 9th International Nanoelectronics Conferences (INEC), Malaysia, (2019)* pp. 1-6.
[8] Gan, N. N. G. M. A., Taib, N. A. M., Abdullah, M., Mukhtar, W. M., & Rashid, A. R. A., "Uric acid detection by using contactless intensity modulation based displacement sensor" in *Journal of Physics: Conference Series, Malaysia,* (2019) p. 012020.
[9] Kamarulzaman, A. H., & Mukhtar, W. M. Science Letters, vol **14**, issue 1(2020) pp. 14-22.
[10] Rashid, A. R. A., Fizi, M. F. M., & Mukhtar, W. M. Journal of Materials in Life Sciences (JOMALISC), **vol** 1, issue 1 (2022) pp. 10-16.
[11] Du, C., Fu, C., Li, P., Meng, Y., Zhong, H., Du, B., ... & He, Journal of Lightwave Technology, vol **41**, issue 5 (2022), pp. 1566-1570.
[12] Mukhtar, W. M., Manaf, N. F. L., & Halim, R. M. ASM Science Journal, vol **15** (2021) pp. 1-8.
[13] Li, M., Singh, R., Marques, C., Zhang, B., & Kumar, S. Optics Express, vol **29**, issue 23 (2021) pp. 38150-38167.

[14] Mukhtar, W. M., & Zailani, N. S. M., "Study on the Sensitivity of Bare Fiber Bragg Grating for Ultrasonic Frequencies Response Under Various Temperature" in *Journal of Physics: Conference Series*, Malaysia, (2020) p. 012013.
[15] Mukhtar, W. M., & Nuraddin, N. A. Optoelectron. Adv. Mat. vol **15**, issue 11-12 (2021) pp. 564-571.
[16] Kumar, V., Raghuwanshi, S. K., & Kumar, S. IEEE Sensors Journal, vol **2**, issue 15 (2022) pp. 14696- 14707.
[17] Mukhtar, W. M., Shaari, S., Ehsan, A. A., & Menon, P. S. Optical Materials Express, vol. 4, issu 3 (2014) pp. 424-433.
[18] Omar, N. A. S., Fen, Y. W., Abdullah, J., Mustapha Kamil, Y., Daniyal, W. M. E. M. M., Sadrolhosseini, A. R., & Mahdi, M. A. Scientific Reports, vol. **10**, issue 1(2020) pp. 2374.
[19] Mukhtar, W. M., "E-coli identification using Kretschmann-based Ag/GO nanocomposites plasmonic sensor", in *AIP Conference Proceedings*, Malaysia, (2020) pp. 020002.
[20] Wang, R., Liu, C., Wei, Y., Jiang, T., Liu, C., Shi, C., Zhao, X., & Li, L. Optik, vol. **266** (2022), pp. 169603.
[21] Teng, C., Shao, P., Li, S., Li, S., Liu, H., Deng, H., Chen, M., Yuan, L.& Deng, S. Optics Communications, vol. **525** (2022) pp. 128844.
[22] Mukhtar, W. M., & Kamarolzaman, I. Journal of Mechanical Engineering and Sciences, vol. **14**, issue 4 (2020) pp. 7540-7550.
[23] Gao, J. W., Wang, D. N. & Xu B. IEEE Photonics Technology Letters, vol. **35**, issue 17 (2023) pp. 935 – 938.
[24] Keiser, G. (2013). Optical Fiber Communications. India: McGraw-Hill Education (India) Private Limited.